

# VORTEX-INDUCED VIBRATION OF TWO TANDEM CYLINDERS NEAR A SURFACE

Jeyson Ferreira Alves<sup>1</sup>, Juan Pablo Julca Avila<sup>2</sup>

<sup>1</sup> Universidade Federal do ABC. Av. dos Estados, 5001, Bangu. CEP: 09210-580. Santo André, SP, Brazil.

jeyson.alves@ufabc.edu.br

<sup>2</sup> Universidade Federal do ABC. Av. dos Estados, 5001, Bangu. CEP: 09210-580. Santo André, SP, Brazil.

juan.avila@ufabc.edu.br

*Abstract: Subsea pipelines when installed on irregular ground, present the free span scenery and suffer from sea current actions. Due to these free spans, the vortex-induced vibration (VIV) phenomenon occurs, which causes fatigue in the structures and compromises the service life of the ducts. In this work, the commercial software ANSYS FLUENT was used to study the hydrodynamic coefficients. For the simulations two cylinders were used in tandem for a distance of 3 diameters,  $D$ , of the cylinder, and the Reynolds number was  $2 \times 10^4$ . The distances between the cylinders and the surface are represented by the ratio  $e/D$ , and this was varied in the range of  $1 < e/D < 0.1$ . The results showed that for reasons  $e/D > 1$  the wall does not influence the results. For reasons  $0.3 < e/D < 0.1$  there is no interaction between the shear layers and, therefore, there is no vortex detachment. In general, good results were obtained for the hydrodynamic coefficients.*

*Keywords: Computational Fluid Dynamics, vortex-induced vibration, subsea pipeline, free span.*

## 1. INTRODUCTION

The world economy has been heavily dependent on the oil market. The influence of this branch on the financial structure of some countries is so great that it can determine their financial rise or decline, especially those in which they are partially or totally dependent on oil exploration and production activities. Brazil is one of these countries, because it has one of the largest and most extensive fields of exploration in the world. Thus, with the successive need to increase oil and gas production over the years, there was a focus on studies for the drilling, exploration, production and transportation of oil in deep and ultra deep waters.

It is often necessary to cause underwater ducts to pass through very irregular areas by subjecting parts of them to free span which can cause structural safety problems. With the extraction in deeper and deeper waters, the vortex-induced vibration becomes a major challenge in ocean structures projects (Santos, 2015).

Static and dynamic loads occur naturally due to the current through the sections of ducts in free spaces. Due to the induced hydrodynamic loads, the ducts can oscillate in-line, producing a drag force ( $F_D$ ) and oscillate in the cross-flow direction, producing a lift force ( $F_L$ ), which are responsible for the phenomenon known as Vortex Induced Vibration (VIV). Such a phenomenon can cause fatigue of the structure and reduce the life of the pipelines, thus directly affecting the production of oil platforms. By means of numerical simulations, (Arakaki Junior, 2016) showed that the drag and lift forces increase when speed increases, while the coefficient values of these forces decrease.

Many studies (Borazjani & Sotiropoulos, 2009; Triyogi Yuwono et al, 2011; Kalvig, 2015; Tang et al, 2015 and Wang et al., 2017) have been conducted in the past, regarding two cylinders in tandem close to a wall, under the incidence of a water current. The main conclusion obtained by these studies is that suppression of vortex detachment occurs when the cylinders approach the wall in a region known as the critical zone.

When the cylinders are at a distance ratio a  $e/D$  less than 0.3, vortex suppression occurs. Experiments conducted by (Arakaki Junior, 2016) with  $R = 2 \times 10^4$  presented suppression of vortex shedding for  $e/D = 0.3$  and the surface allowed to influence the results for  $e/D > 1$ . The suppression of vortex shedding is due to the following factors: the cylinder stagnation point moving to a position closer to the wall, the angular change of the vortex separation point and also due to the pressure distribution of asymmetry. Therefore, when submarine ducts are in free-sided condition with very small ratios  $e/D$ , partial or complete suppression of vortex shedding occurs.

In this work, the development of numerical modeling and two-dimensional flow simulations of two cylinders in tandem near a surface, with free vibration was done by commercial CFD software ANSYS FLUENT. The simulations were performed for the case where where the downstream cylinder oscillates and the upstream cylinder remains stationary. The reasons for the spacing between the cylinders and the surface were varied. For the discretization of the transport equations, this software uses the Finite Volumes Method. In order to study the hydrodynamic coefficients of the cylinders, a Reynolds number equal to  $2 \times 10^4$  and the SST  $k-\omega$  turbulence model were chosen. For the pressure-velocity coupling solution the SIMPLE algorithm was employed.

## 2. COMPUTATIONAL FLUID DYNAMICS EQUATIONS

### Numerical method

The vortex shedding is related to the Reynolds number as in Eq. (1) and the Strouhal number expresses a relationship between vortex shedding frequency,  $f_v$  the cylinder diameter,  $D$ , and the flow velocity of the fluid,  $U$ , as in Eq. (2)

$$R_e = \frac{DU}{\nu} \quad (1)$$

$$S_t = \frac{f_v D}{U} \quad (2)$$

where,  $\nu$  is the kinematic viscosity and  $St$  is the Strouhal number.

The lift force is directly related to the frequency of vortex shedding. When the cylinder moves in the cross-line direction, oscillations in the drag coefficient occur. Mean drag and lift coefficients are defined by Eqs. (3) and (4):

$$C_D = \frac{F_D}{(1/2)\rho U^2 D} \quad (3)$$

$$C_L = \frac{F_L}{(1/2)\rho U^2 D} \quad (4)$$

in which,  $\rho$ =fluid density,  $F_D$  and  $F_L$  are mean drag and lift forces, respectively.

The tendency is that the drag coefficient decreases as the  $e/D$  ratio decreases. The Figure 1 shows the results obtained experimentally by Roshko (1975) and Zdravkovich (1985) for different numbers of Reynolds.

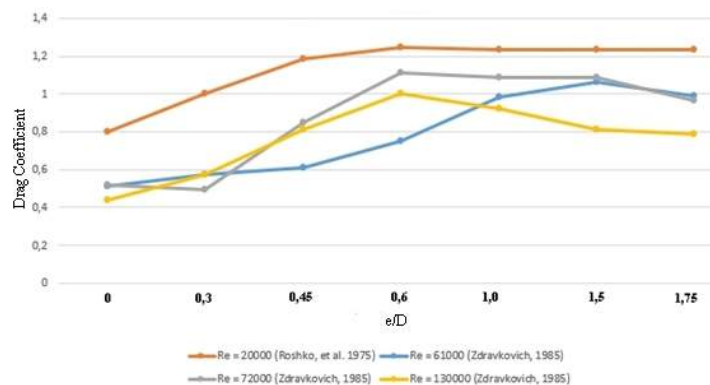


Figure 1 - Cylinder drag coefficient near to the wall.

As can be seen, the drag coefficient increases when there is an increase in the ratio  $e/D$ , but for high ratios  $e/D$  the drag coefficient tends to remain constant.

Experiments performed by Fredsøe and Hansen (1987), Kok (1988) and Sumer and Fredsøe et al. (2006) on the average lift coefficient of a cylinder near a wall show that the lift decreases for high ratios of  $e/D$ , reaching zero, and presents a considerable increase when this ratio decreases. According to Arakaki-Junior (2016), this fact is due to the change from the stagnation point to smaller angular positions.

Figure 2 shows values obtained experimentally by Sumer and Fredsøe (2006) of average lift coefficients for different ratios  $e/D$ .

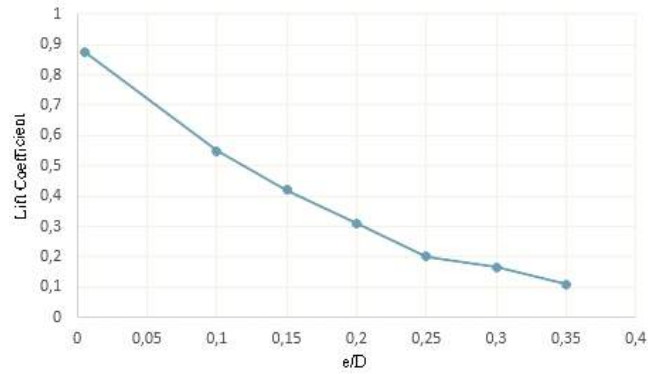


Figure 2 - Experimental results of the lift coefficient with different ratios e/D (Sumer and Fredsøe, 2006).

### 2.1 Governing equations

For a two-dimensional flow, the governing equations for an incompressible Newtonian fluid are the conservation equations of mass Eq. (5) and the equation of conservation of the momentum Eq. (6):

$$\frac{\partial u_i}{\partial x_i} = 0 \tag{5}$$

$$\rho \frac{\partial u_i}{\partial t} + \rho \frac{\partial u_j u_i}{\partial x_j} = -\frac{\partial p}{\partial x_i} + \mu \frac{\partial^2 u_i}{\partial x_j \partial x_j} \tag{6}$$

in which,  $u_i$  are the velocity components in x and y directions.

#### Mathematical model

A simple scheme of a tandem two-cylinder arrangement is shown in Figure 3. The moving rigid cylinder is mounted on an elastic base with one degree of freedom in y-direction. Therefore, the elastic cylinder is a simple mass-damper-spring system and the equation of motion is presented in Eq. (7):

$$m\ddot{y}(t) + c\dot{y}(t) + ky = F(t) \tag{7}$$

In the equation above,  $m$  is the total oscillating mass of system,  $y$  is the normal direction of flow,  $\dot{y}$  and  $\ddot{y}$  are velocity and acceleration of cylinder, respectively,  $c$  is damping coefficient,  $k$  is spring stiffness and  $F$  is the fluid force which is exerted on the cylinder boundary perpendicular to the flow.

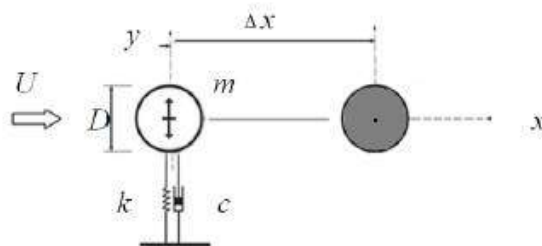


Figure 3 – Schematic of two cylinders in tandem in cross flow, the downstream is free to move; the upstream is rigidly mounted.

### 2.2 Turbulence model

When performing simulation studies the turbulence model is a very important parameter to be chosen, because it will directly affect the results obtained. Although there is still no turbulence model capable of solving all possible runoff conditions, many studies have been carried out with the aim of finding the best model to use in each type of flow.

In this work, the RANS equations were chosen and the most popular models are k- $\omega$  and k- $\epsilon$ . The k- $\epsilon$  model is widely used because it presents good convergence and requires little computational capability, but it can't solve flows

that present adverse pressure gradients. The  $k-\omega$  model solves the equations in the viscous sublayer and presents no stability problems.

Therefore, to solve the problem of this work, the SST  $k-\omega$  model was used because it combines the  $k-\omega$  and  $k-\epsilon$  models and is tested as good in the flows with adverse pressure gradients.

### 2.3 Computational domain, geometry, mesh and boundary conditions

Figure 4 shows the computational domain used in the simulations. A distance between the two cylinders with a value of  $3D$  was set, the distance between the cylinders and the surface,  $e$ , was varied from  $0.1D$  to  $1D$  to evaluate the effects of the wall and the dimensions of the Cartesian axes  $x$  and  $y$  are  $34D$  and  $14D$ , respectively. The diameters used were  $0.01\text{m}$ ,  $\rho = 998.2 \text{ kg / m}^3$  and  $\nu = 10^{-6} \text{ m}^2/\text{s}$ .

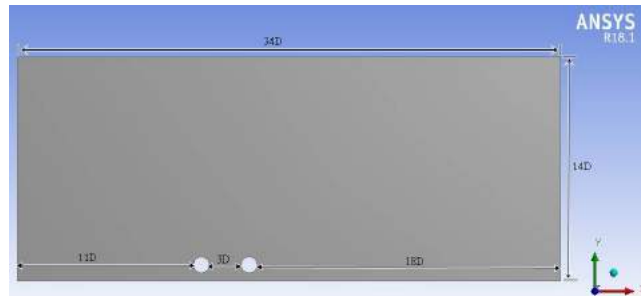


Figure 4 – Computational domain.

The dimensions of the computational domain were the same as those used by (Arakaki Junior, 2016) in such a way that top, entry and exit do not influence the region of interest of this study. The simulations were performed in a bidimensional way due to the computational costs of performing three-dimensional simulations.

Inlet velocity (axis  $x$ ) is set to  $U=2\text{m/s}$  ( $Re=2 \cdot 10^4$ ), and outlet pressure specified is set to zero.

ANSYS ICEM software was used to generate a thin mesh with tetrahedrals to obtain a high quality in the boundary layer. The O-grid method was used around the cylinder in order to avoid distortions of the elements as shown in Figure 5.

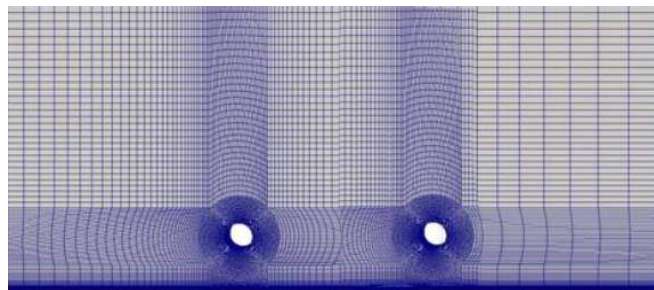


Figure 5 – Refined mesh near the wall and around the tandem cylinders.

## 3. RESULTS

### 3.1 Convergence test

The convergence test is summarized in simulations for each ratio  $e/D$  and to verify the relationship between the number of elements of the computational domain and the values of the drag coefficients.

The test is completed when the value of the drag coefficient stops to change and remains constant regardless of the number of elements of the computational domain. The Figure 6 summarizes the simulations for the different ratios and  $e/D$  and the number of elements used in each simulation.

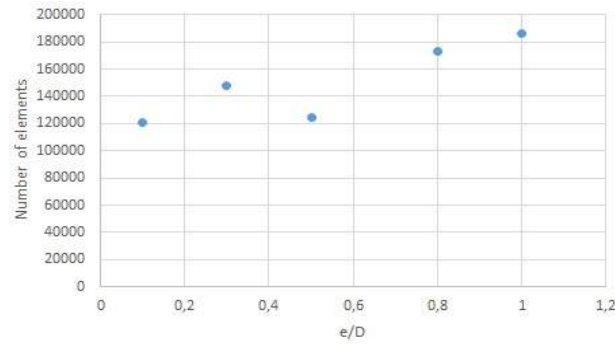


Figure 6 - Number of elements of the simulations.

Most ratios  $e/D$  were made without complications, however, the clearance value presented difficulties 0.1. This response of the simulation is due to the distortion of the elements when the surface cylinder is very close. Therefore, one should not work with very small ratios, because they present problems in convergence test.

All meshes generated in the simulations presented values of  $y^+ < 2$  in the vicinity of the cylinder surface. At the moment the free span reduction occurs, the distances between the cylinder and the wall also decrease, reducing the cells between the two elements, giving meshes with smaller  $y^+$  in the cylinder region as can be seen in the Figure 7.

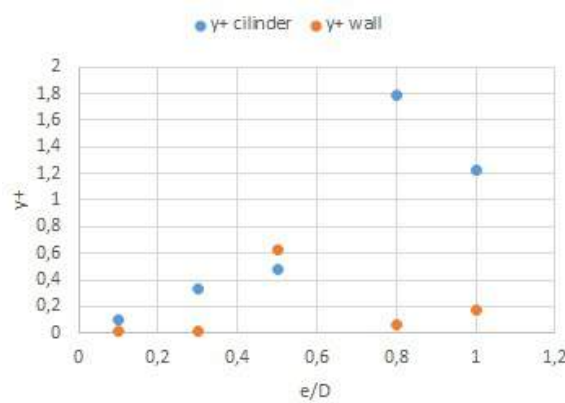


Figure 7 -  $y^+$  of the simulations.

### 3.2 Comparison of the different turbulence models used

Two models of turbulence were tested in the simulations ( $k - \omega$  SST and standard  $k - \epsilon$ ) in order to verify which would present the best results for the  $e / D$  ratios equal to 1; 0.8; 0.5; 0.3 and 0.1.

Using the model studied by Arakaki Junior (2016), comparisons were made between the mean drag and lift coefficients (Table 1), in order to find the error values.

**Table 1 - Results of comparisons between turbulence models with (Arakaki Junior, 2016).**

e/D	k - ε				k - ω SST				Arakaki Junior (2016)	
	$\overline{C_D}$	Error (%)	$\overline{C_L}$	Error (%)	$\overline{C_D}$	Error (%)	$\overline{C_L}$	Error (%)	$\overline{C_D}$	$\overline{C_L}$
0.3	0.98	14	0.24	25	1.14	0	0.32	0	1.14	0.32
0.5	0.98	18	0.13	13.3	1.18	1.66	0.17	13.33	1.20	0.15
0.8	0.77	41.2	0.03	70	1.33	1.53	0.10	0	1.31	0.10
1	0.85	35	0.07	22.2	1.18	9.9	0.80	11	1.31	0.09

The experimental values of Arakaki Junior (2016) had already been compared with those taken from graphs by Roshko et al. (1975), and he had come to the conclusion that the results made using the k-ω SST model presented closer results in the literature. In this paper the presented results also approximated those found in the literature for the great majority of the cases studied.

Therefore, the simulations performed also used the turbulence model k-ω SST. Another important feature of this model is its ability to solve flows with adverse pressure gradients, as in the flow of the present work.

The meshes were generated with values of  $y^+ < 2$  in the vicinity of the cylinder and the wall. At the moment the free span is reduced, the intervals between the cylinder and the wall also decrease, reducing the cells between the two elements, giving meshes with  $y^+$  smaller in the region of the cylinder.

In this work the effects of the boundary layer in the flow corresponding to the friction with the wall were not taken into account. According to Neto (2012), the ratio e/D governs the flow characteristics.

### 3.3 Drag and lift coefficients in a turbulent flow with $Re=2 \times 10^4$ for different value of e/D

Simulations performed using commercial ANSYS FLUENT software were made in the range of  $0.1 < e/D < 1$ .

$e/D = 1$

When studying the flow around cylinders with ratios e/D equal to 1 it was possible to observe the non-occurrence of influence of the wall, since the flow acts as if the cylinders were oscillating without the presence of a wall. It is possible to observe the detachment of vortices as well as the formation of the mat, as portrayed in the literature. The same behavior is noted for ratios e/D, greater than 1.

The velocity magnitude contours and time history of drag and lift coefficients for e/D=1 are represented in Figures 8, 9 (a) and 9 (b).

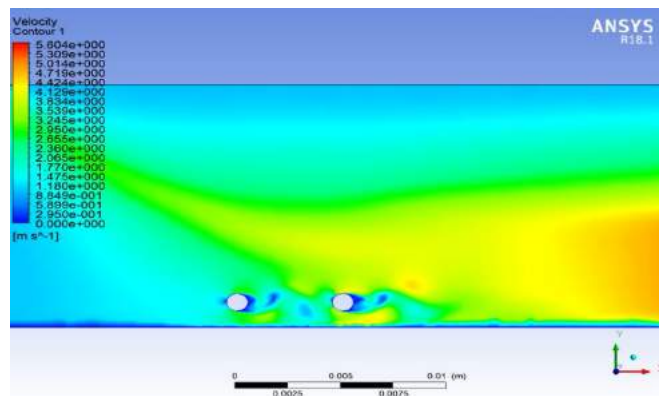


**Figure 8 – Flow visualization for e/D = 1.**

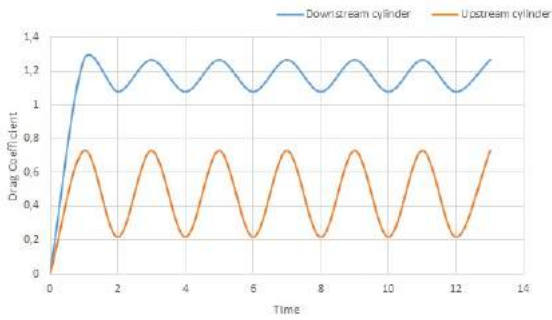


Figure 9 (a) – Time history of drag coefficients.

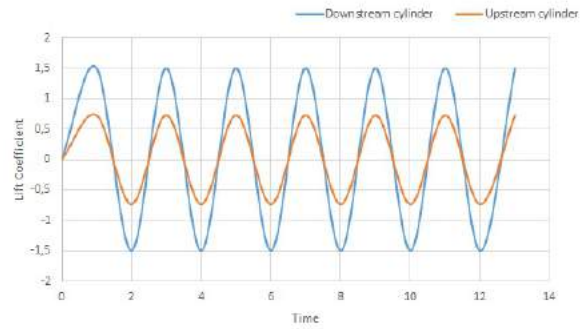


Figure 9 (b) – Time history of lift coefficients.

In the simulation it was observed that the vortices are alternately detached as described in the literature. Through post-processing it is possible to see the magnitude of the flow velocity field, as shown in Figure 8. The flow colors reproduce velocity scales, the colors of which are close to the blue ones with the lowest velocities and those close to the red ones with the higher velocities.

$e/D = 0.8$

Analogously to  $e/D = 1$ , the flow with  $e/D = 0.8$  is basically not under the influence of the wall. As can be seen in Figure 10, is the alternating vortex shedding and training mat.

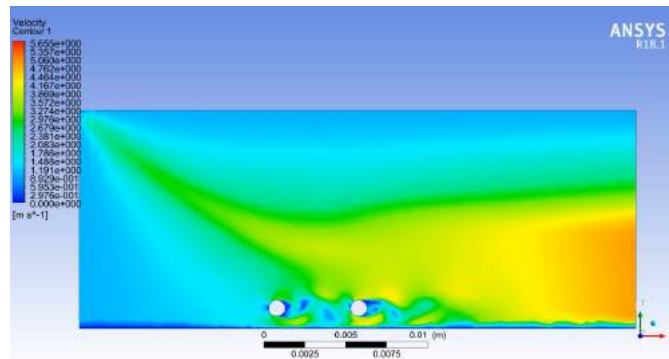


Figure 10 - Flow visualization for  $e/D = 0.8$ .

It is expected that with this reason changes in the flow occur because the cylinders are closer to the wall. However, the values of the drag and lift coefficients practically did not change when compared to the  $e/D$  equals 1. The values of the drag and lift coefficients for this flow can be observed in Figures 11 (a) and 11 (b).

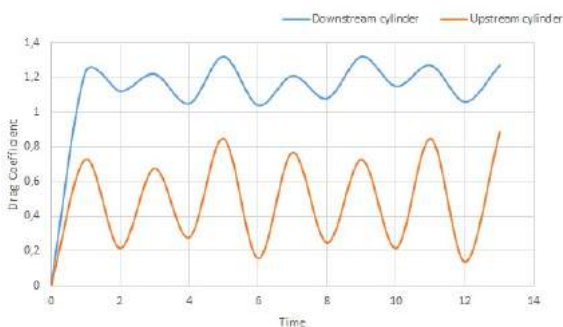


Figure 11 (a) – Time history of drag coefficients.

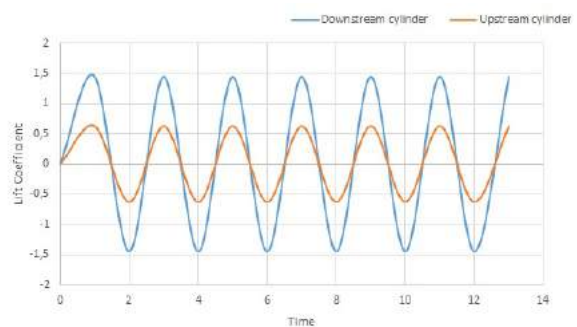


Figure 11 (b) – Time history of lift coefficients.

$e/D = 0.5$

Suppression of the vortices for the ratio equal to 0.5 does not occur yet. There is a less developed shear layer on the side of the wall compared to the free sides of the cylinders, providing a weaker interaction between the layers. Such

### Vortex-induced vibration of two tandem cylinders near a surface

interaction decreases as the cylinders approach the surface. Figure 12 is the flow visualization for this ratio and Figure 13 (a) and 13 (b) is the time history of the time history to hydrodynamics coefficients.

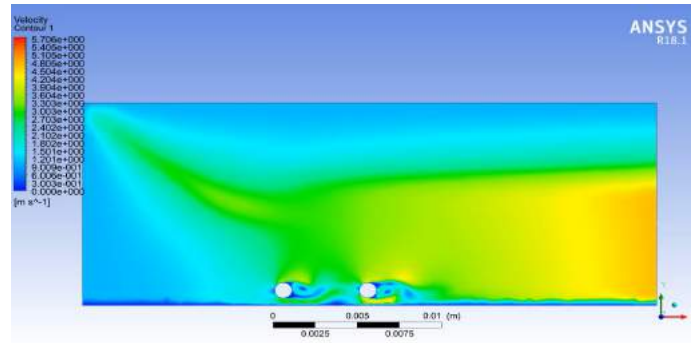


Figure 12 – Flow visualization for  $e/D = 0.5$ .

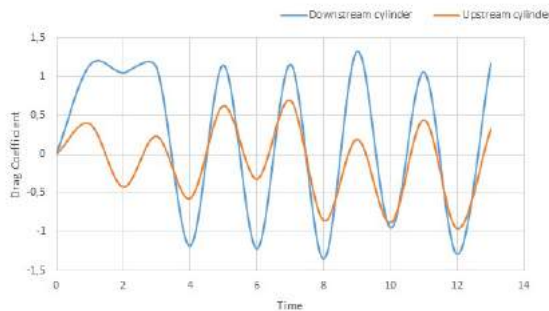


Figure 13 (a) – Time history of drag coefficients.

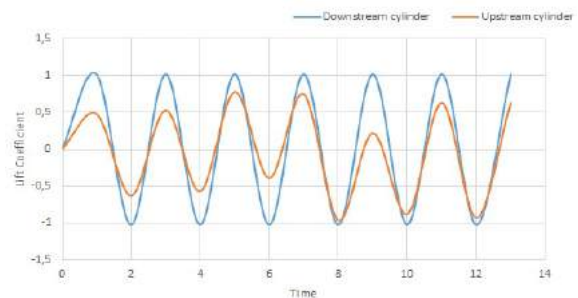


Figure 13 (b) – Time history of lift coefficients.

With this ratio it is already possible to observe the wall influencing the flow. It is already possible to observe a reduction of interaction of the boundary layers. Still no suppression of the emission of vortices occurs.

### $e/D = 0.3$

For the ratio  $e/D$  equal to 0.3, a reduction of the interaction between layers both bottom and top cylinders, causing vortices to be suppressed in the lower region of the cylinders. It is possible to see a partial suppression of vortex shedding because of this being in a region called the critical zone. For the determination of the critical zone, simulations were performed for ratios in the range of  $0.1 < e/D < 0.3$ , where it is possible to observe that from this range, the suppression of vortices starts. Figure 14 is the flow visualization and the Figures 15 (a) and 15 (b) is the time history of drag and lift coefficients.

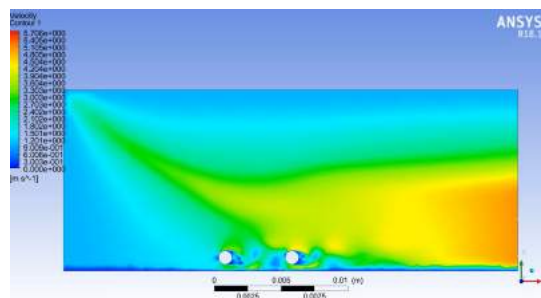


Figure 14 - Flow visualization for  $e/D = 0.3$ .

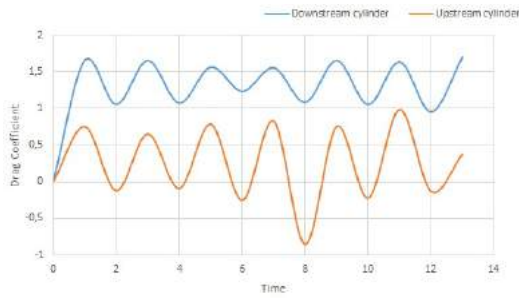


Figure 15 (a) – Time history of drag coefficients.

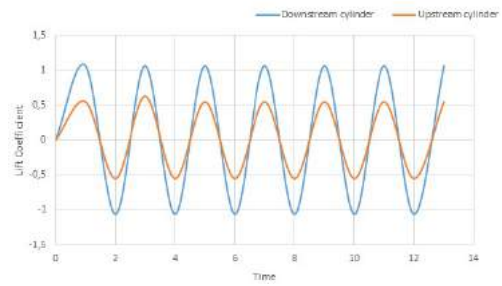


Figure 15 (b) – Time history of lift coefficients.

$e/D = 0.1$

There is no interaction between the cylinder shear layers and the suppression occurs complete the vortices. Figure 16 shows the contour of the velocity field magnitude, indicating that the detachment was actually suppressed due to the low fluid flow in the lower region of the cylinder, creating an enormous vortex downstream of the cylinder, analogous to that observed empirically by Price et al. (2002).

Figures 17 (a) and 17 (b) show the sign of the drag and lift coefficients. It is possible to notice that there are no changes of the coefficients that remain in a constant value, which is the result of the suppression of vortices.

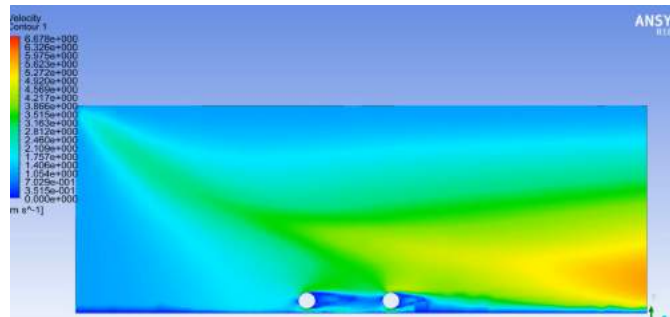


Figure 16 - Flow visualization of  $e/D = 0.1$ .

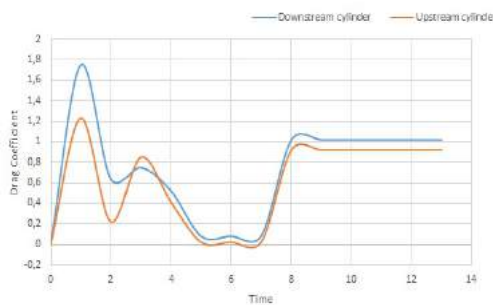


Figure 17 (a) – Time history of drag coefficients.

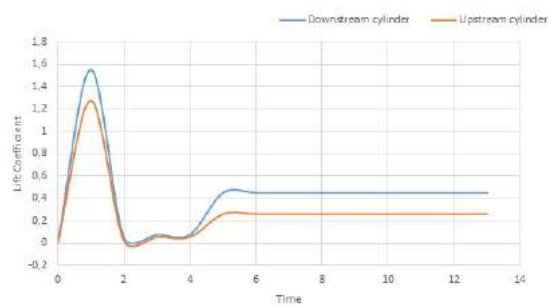


Figure 17 (b) – Time history of lift coefficients.

#### 4. CONCLUSIONS

By means of computational fluid dynamics it was possible to study the coefficients hydrodynamics of the cylinders near a rigid surface. The history of the hydrodynamic coefficients was studied and compared with results from the literature.

It was possible to notice that the choice of the mesh to be used in the simulations directly the results of the hydrodynamic coefficients, since a more refined mesh can approach the real conditions of the problem, thus obtaining values of the hydrodynamic coefficients close to the real values.

Due to the studied problem presenting adverse pressure gradients, the turbulence model that best represented the hydrodynamic coefficients was the SST  $k-\omega$  model.

For studies of tandem pipelines close to a surface, it is not only the ratio  $e/D$  that influences the flow, but also the distance at which the ducts are positioned. For reasons  $0.3 < e/D < 0.1$  it is noted that partial or complete deletion of vortices occurs.

The ANSYS FLUENT software accurately reproduced the hydrodynamic coefficients in the submarine pipelines. With its post-processing it was possible to better understand the results thanks to the speed contours. Thus, it was possible to better understand the experimental results found in the literature.

## REFERENCES

- Arakaki Junior, H., 2016, "Estudo dos esforços de correnteza marítima em risers com uso de CFD". MSc dissertation, Campinas State University, Campinas.
- Borazjani, I., Sotiropoulos, F., 2009, "Vortex-induced vibrations of two cylinders in tandem arrangement in the proximity-wake interference region", *Journal of Fluid Mechanics*, Vol. 621, pp. 321-364.
- Fredsøe, J., Hansen, E., 1987. "Lift forces on pipelines in steady flow". *Journal of Waterway, Port, Coastal and Ocean Eng.*, Vol. 113, p. 139-155.
- Kalvig, R. H., 2015, "Numerical investigation of 3D flow around two tandem cylinders". MSc dissertation, Norwegian University of Science and Technology, Trondheim.
- Kok, N. J., 1998, "Lift and Drag Processes on a Submarine Pipeline in Steady Flow". Doc dissertation, Department of Civil Engineering, University of Cape Town, Cape Town.
- Neto, M. C., 2012, "*Simulação numérica bidimensional do escoamento ao redor de um cilindro circular próximo a uma placa plana*", MSc dissertation, Federal University of Rio de Janeiro, Rio de Janeiro.
- Price, S.J., Sumner, D., Smith, J.G., Leong, K., Paidoussis, M.P., 2002. "Flow visualization around a circular cylinder near to a plane wall". *Journal of Fluids and Structures*, Vol. 16, p. 175-191.
- Roshko, A., Steinolfson, A., Chattoroon, V., 1975. "Flow forces on a cylinder near a wall or near another cylinder", In *Proceeding of the 2nd US Conference Wind Engineering Research Colorado*, USA.
- Santos, M. V. F., 2015, "Um estudo comparativo de dutos em vãos livres através de simulações numéricas". MSc dissertation, Campinas State University, Campinas.
- Sumer, B.M., Fredsøe, J., 2006. *Hydrodynamics Around Cylindrical Structures*. World Scientific Publishing Co. Pte Ltd, Singapore, Revised edition.
- Wang, X. K., Hao, Z., Zhang, J. X., Tan, S. K., 2017, "Flow around two tandem square cylinders near a plane wall", *Experiments in Fluids*, Vol. 55, pp. 1818-1832.
- Yuwono, T., Widodo, W. A., Mirmanto, H., Fahreza, F., 2011, "Plane wall effect of flow around two circular cylinders in tandem arrangement", *The Journal for Technology and Science*, Vol. 22, pp. 1-6.

## RESPONSIBILITY NOTICE

The author(s) is (are) the only responsible for the printed material included in this paper.